*Am J Physiol Renal Physiol* 293: F994–F1006, 2007.
First published June 20, 2007; doi:10.1152/ajprenal.00114.2007.

# Proteomics of *S*-(1, 2-dichlorovinyl)-L-cysteine-induced acute renal failure and autoprotection in mice

**Midhun C. Korrapati,[1] Jaya Chilakapati,[1] Frank A. Witzmann,[2] Chundury Rao,[2] Edward A. Lock,[3] and Harihara M. Mehendale[1]**

[1]*Department of Toxicology, College of Pharmacy, University of Louisiana Monroe, Monroe, Louisiana;* [2]*Department of Cellular and Integrative Physiology, Indiana University School of Medicine, Biotechnology Research and Training Center, Indianapolis, Indiana; and* [3]*School of Biomolecular Sciences, Liverpool John Moores University, Liverpool, United Kingdom*

Submitted 6 March 2007; accepted in final form 6 June 2007

**Korrapati MC, Chilakapati J, Witzmann FA, Rao C, Lock EA, Mehendale HM.** Proteomics of *S*-(1, 2-dichlorovinyl)-L-cysteine-induced acute renal failure and autoprotection in mice. *Am J Physiol Renal Physiol* 293: F994–F1006, 2007. First published June 20, 2007; doi:10.1152/ajprenal.00114.2007.—Previous studies (Vaidya VS, Shankar K, Lock EA, Bucci TJ, Mehendale HM. *Toxicol Sci* 74: 215–227, 2003; Korrapati MC, Lock EA, Mehendale HM. *Am J Physiol Renal Physiol* 289: F175–F185, 2005; Korrapati MC, Chilakapati J, Lock EA, Latendresse JR, Warbritton A, Mehendale HM. *Am J Physiol Renal Physiol* 291: F439–F455, 2006) demonstrated that renal repair stimulated by a low dose of *S*-(1,2-dichlorovinyl)-L-cysteine (DCVC; 15 mg/kg ip) 72 h before administration of a normally lethal dose (75 mg/kg ip) protects mice from acute renal failure (ARF) and death (autoprotection). The present study identified the proteins indicative of DCVC-induced ARF and autoprotection in male Swiss Webster mice. Renal dysfunction and injury were assessed by plasma creatinine and histopathology, respectively. Whole-kidney homogenates were run on two-dimensional gel electrophoresis gels, and the expression of 18 common proteins was maximally changed ($\geq$10-fold) in all the treatment groups and they were conclusively identified by liquid chromatography tandem mass spectrometry. These proteins were mildly downregulated after low dose alone and in autoprotected mice in contrast to severe downregulation with high dose alone. Glucose-regulated protein 75 and proteasome $\alpha$-subunit type 1 were further investigated by immunohistochemistry for their localization in the kidneys of all the groups. These proteins were substantially higher in the proximal convoluted tubular epithelial cells in the low-dose and autoprotected groups compared with high-dose alone group. Proteins involved in energetics were downregulated in all the three groups of mice, leading to a compromise in cellular energy. However, energy is recovered completely in low-dose and autoprotected mice. This study provides the first report on proteomics of DCVC-induced ARF and autoprotection in mice and reflects the application of proteomics in mechanistic studies as well as biomarker development in a variety of toxicological paradigms.

autoprotection; DCVC-induced renal failure; glucose regulated protein 75; proteasome $\alpha$-subunit type 1

ACUTE RENAL FAILURE (ARF) is a clinical syndrome characterized by a rapid decline in glomerular filtration rate and is associated with high morbidity and mortality rates; however, it is potentially reversible if patients are free from life-threatening complications (52). Acute tubular necrosis (ATN) with prerenal disease is the most common cause of ARF, accounting for two-thirds of intrinsic causes (18). ATN is characterized by a regeneration phase (30), which is very important as it leads to recovery of renal function. Recovery from ARF-bound renal injury relies on a sequence of events, including epithelial cell dedifferentiation and proliferation followed by differentiation and finally, restoration of the functional integrity of the nephron (1). Although the morphological characteristics of the repair process have been described (69), the molecular regulation of the events leading to regeneration after ATN is not completely understood (55). Over the last three decades, work with several experimental models has made it possible to identify the pathophysiological mechanisms associated with ARF and has enhanced our understanding of the disease (33, 48, 63, 64). The pathophysiology of DCVC-induced ATN followed by ARF in mice and clinical ARF in patients is similar (14, 23, 27–30). Therefore, a greater understanding of the potential mechanisms of ATN and ARF by using models like DCVC-induced autoprotection is needed. Although our understanding of the mechanisms of recovery from ARF-bound injury is limited (24, 39), early detection and intervention to stimulate renal tubular repair to restore the structure and function may lead to reductions in mortality rates. Therefore, understanding the mechanisms of renal tissue repair is critical to the development and evaluation of pharmacological strategies to prevent and/or treat ARF.

Previously, we have shown that proximal tubular injury initiated by a lethal high dose of DCVC progresses because cell division and renal tissue repair are inhibited, leading to ARF and death in mice (64). Proximal tubular injury initiated by low to moderate doses of DCVC is repaired by timely and adequate stimulation of cell division and renal tissue repair, restoration of renal structure and function, and survival of mice by averting ARF-bound injury.[1] Nephro-autoprotection is characterized by prior administration of a low dose of DCVC, which primes renal cell division such that tissue repair is no longer inhibited even after exposure to a normally lethal dose of DCVC (28, 64, 65). The critical role of cellular signaling

[1] ARF due to high dose of DCVC is a lethal disease because renal tissue repair is inhibited by this high dose. In the absence of tissue repair, high dose-induced renal injury progresses culminating in ARF and death. An intervention such as priming with low dose of DCVC (autoprotected group) prevents high dose-induced ARF despite massive injury, indicating the possibility of averting the end-stage disease. In this paper, the course of progression of renal injury until successful avertion to keep it from reaching the end stage can be referred to as ARF-bound injury.

Address for reprint requests and other correspondence: H. M. Mehendale, Dept. of Toxicology, College of Pharmacy, Univ. of Louisiana Monroe, 700 Univ. Ave., Sugar Hall 306, Monroe, LA 71209-0470 (e-mail: mehendale@ulm.edu).

The costs of publication of this article were defrayed in part by the payment of page charges. The article must therefore be hereby marked "*advertisement*" in accordance with 18 U.S.C. Section 1734 solely to indicate this fact

mechanisms in stimulating renal cell division and sustaining renal tissue repair in the autoprotection model has been documented (27, 28, 66). However, understanding compensatory mechanisms other than cell division is also important to identify and profile the critical molecular biomarkers of renal injury and repair following ARF-bound injury to develop potential therapeutic measures.

Proteomic studies are envisioned to help in the translation of genomics to clinically useful applications, especially in the areas of diagnostics and prognostics (41, 70). In the diagnosis and treatment of kidney disease, the identification of disease-associated early biomarkers is a major priority. Proteomics, with its high-throughput and unbiased approach to the analysis of variations in protein expression patterns, promises to be the most suitable platform for biomarker discovery (34, 40, 42, 74). Combining such classic analytic techniques as two-dimensional gel electrophoresis with more sophisticated techniques, such as mass spectrometry (MS) has made it possible to catalog and quantify proteins present in urine and various kidney tissue compartments in both normal and diseased physiological states. However, information on proteins associated with injury and recovery mechanisms following ARF-bound injury in appropriate animal models is scarce. The present study presents for the first time proteomic profiling of various proteins following DCVC-induced renal damage and autoprotection in mice.

## METHODS

*Reagents.* Unless stated otherwise, all chemicals and biochemicals were purchased from Sigma (St. Louis, MO). DCVC was provided by Syngenta (Central Toxicology Laboratory, Macclesfield, Cheshire, UK) and was >99.5% pure. 3,3′-Diaminobenzidine tetrahydrochloride was purchased from Dako (Carpinteria, CA). Ultrapure electrophoretic reagents were obtained from Bio-Rad (Richmond, CA), Sigma (Poole, UK), and National Diagnostics (Atlanta, GA). Sequence-grade trypsin was obtained from Roche Molecular Biochemicals (Indianapolis, IN). 3-[(3-Cholamidopropyl)dimethylammonio]-1-propanesulfonate and dithiothreitol were obtained from Calbiochem (La Jolla, CA), and *N*-isopropyl iodoacetamide from Molecular Probes (Eugene, OR).

*Animals and treatment.* Male Swiss Webster (SW) mice (25–29 g) were purchased from Harlan Sprague-Dawley (Indianapolis, IN) and were maintained in our central animal facility under 21 ± 1°C temperature and 50 ± 10% relative humidity at all times. They were maintained on a 12:12- h light-dark cycle over wood chips free of any known chemical contaminants. The mice received commercial rodent chow (Teklad rodent diet 7012) and water ad libitum and were acclimated for 1 wk before use. All animal maintenance and treatment protocols were in compliance with the *Guide for the Care and Use of Laboratory Animals* as adopted and promulgated by the US National Institutes of Health and were approved by our Institutional Animal Care and Use Committee.

*Lethality study.* To confirm our previous findings, a lethality study was conducted with mice which were divided into four groups ($n$ = 10/group). Mice in *groups I* and *III* were injected with distilled water (DW; 10 ml/kg) on *day 0* followed by DW (10 ml/kg; *group I*) or high-dose DCVC (75 mg/kg ip; *group III*) in DW (10 ml/kg) at 72 h, respectively. *Groups II* and *IV* received low-dose DCVC (15 mg/kg ip) in DW (10 ml/kg) on *day 0* followed by either 10 ml/kg DW ip (*group II*) or high-dose DCVC (75 mg/kg ip) in DW (10 ml/kg) at 72 h (*group IV*; autoprotection group), respectively. Mice were observed twice daily for 14 days, and survival/mortality data were recorded. All deaths occurred between 36 and 48 h after the high dose of DCVC in *group III*.

*Time course study.* A separate study was conducted with mice from *groups I*, *II*, *III*, and *IV*. *Groups I*, *II*, and *IV* had three mice per time point ($n$ = 3). *Group III* consisted of five mice to ensure a minimum of three surviving mice, because mice started dying between 108 and 120 h (36–48 h after the high dose) in the lethality experiment (Table 1). Mice were terminated under diethyl ether anesthesia at 6, 12, 24, 36, 72, 78, 84, 96, 144, 240, and 336 h after the low-dose administration in *groups II* and *IV*. Mice in *group III* ($n$ = 3/time point) were terminated after the administration of DW at 6, 12, 24, 36, 72, 78, 84, 96, and 108 h. Plasma was collected from mice at each time point to assess renal function. Kidneys were also isolated from these mice at each time point after respective treatment for further analysis of renal ATP content, histopathology, and immunohistochemical staining. In addition, kidneys isolated from mice in all the groups at 36 h were also used for running two-dimensional gel electrophoresis (2-DE). Previous studies have shown that 90% of the mice receiving only the high dose of DCVC (*group III*) die between 108 and 120 h (36–48 h after the high dose) after DW administration (64, 65). For proteomic studies, a 36-h time point after DW or DCVC was selected for 2-DE. The objective for selecting a 36-h time point after DW (*group I*) or DCVC (*group II*, second treatment of DCVC in *groups III* and *IV*) for proteomic studies was to identify key protein modifications before animal death in *group III* (high-dose group). In addition, we selected the same time point after high dose in *group IV* (autoprotected group) to examine protein modifications during recovery from DCVC-initiated injury, ARF, and death.

*Plasma enzymes.* Plasma was separated by centrifugation. Creatinine levels (catalog no. 63–25, Sigma; procedure 63-UV) were measured as a biomarker for renal dysfunction using a commercially available kit (Sigma). Plasma creatinine levels were measured over a time course in *groups II*, *III*, and *IV*.

*Renal histopathology.* Portions of the kidneys that were removed from mice at 36 h after the treatment with either DW (*group I*, controls) or DCVC (*group II*, second treatment of DCVC in *groups III* and *IV*) was used for assessing renal injury by histopathology, and the remaining kidney tissue was used to make homogenates for proteomic analysis by 2-DE and measurement of ATP content. To find whether changes in protein expression at 36 h after respective treatments with DCVC reflect renal damage, these sections were used to confirm renal damage by histopathology. Kidneys from control and treated mice were washed with ice-cold normal saline (0.9% NaCl), cut transversely into thin slices, and then fixed into 10% neutral-buffered formaldehyde for 48 h. The tissues were then transferred into 70% ethyl alcohol, processed, and embedded in paraffin wax. Kidney sections (4-μm thin) were stained with hematoxylin and eosin for histological examination under a light microscope. Three ×200 microscopic fields were randomly chosen from the corticomedullary

Table 1. *DCVC autoprotection in male SW mice*

| Treatment Group | Treatment and Sequence | No. of Mice: Total | No. of Mice: % Mortality | Time of Death,* h |
|---|---|---|---|---|
| *Group I* | DW+DW | 10 | 0 | |
| *Group II* | Low dose+DW | 10 | 0 | |
| *GroupIII* | DW+high dose | 10 | 90 | 36–48 |
| *GroupIV* | Low dose+high dose | 10 | 0 | |

SW, Swiss Webster; DW, distilled water. Mice in *groups I* and *III* were injected with distilled water (DW; 10 ml/kg) on *day 0* followed by DW (10 ml/kg, *group I*) or high-dose *S*-(1, 2-dichlorovinyl)-L-cysteine (DCVC; 75 mg/kg ip) in DW (10 ml/kg, *group III*) at 72 h, respectively. *Groups II* and *IV* received a low dose (15 mg DCVC/kg ip) in DW (10 ml/kg) on *day 0* (*group II*) followed by either 10 ml/kg DW ip (*group II*) or a high dose (75 mg DCVC/kg ip) in DW (10 ml/kg) at 72 h (*group IV*), respectively. Mice were observed twice daily for 14 days, and survival/mortality data were recorded. All deaths occurred between 36 and 48 h after the high dose of DCVC in *group III*. *Time after the second treatment.

region (CMR) encompassing the outer stripe of outer medulla (OSOM) from each mouse ($n = 3$/group); the CMR encompassing the OSOM is the principal region of the nephron damaged by DCVC. Tubules were considered necrotic if they were lined with profiles of amorphous cells with coagulated eosinophilic cytoplasm and ghostly silhouettes of karyolitic nuclei or exfoliated cells, detritus, or both.

*Sample preparation.* Whole-kidney homogenates were made using kidneys that were isolated from mice at 36 h after the treatment with either DW (*group I*, controls) or DCVC (*group II*, second treatment of DCVC in *groups III* and *IV*). Kidney tissue was placed in a 50-ml beaker, along with eight volumes of a solution containing 9 M urea, 4% Igepal CA-630 ([octylphenoxy] polyethoxyethanol), 1% DTT, and 2% carrier ampholytes (pH 8–10.5), and thoroughly minced with surgical scissors. The minced samples were then placed in 3-ml DUALL (Kimble/Kontes, Vineland, NJ) ground-glass tissue grinders and manually homogenized. After solubilization at room temperature for 120 min, samples were centrifuged at 100,000 *g* for 30 min using a Beckman (Fullerton, CA) TL-100 ultracentrifuge to remove nucleic acid and insoluble materials; the supernatants were stored at −45°C until 2-DE separation.

*2-DE.* Using overnight, passive rehydration at room temperature, 500 μg protein from all the samples in all groups was loaded onto IPG strips (24 cm, nonlinear pH 3–10, Bio-Rad, Hercules, CA). Isoelectric focusing was performed simultaneously on all IPG strips randomly assigned to two Protean IEF Cells (10 strips/instrument, Bio-Rad) by a program of progressively increasing voltage (150 V for 2 h, 300 V for 4 h, 1,500 V for 1 h, 5,000 V for 5 h, 7,000 V for 6 h, and 10,000V for 3 h) for a total of 100,000 V/h. A computer-controlled gradient casting system was used to prepare second-dimension (2-D) SDS gradient slab gels (20 × 25 × 0.15 cm) in which the acrylamide concentration varied linearly from 11 to 17% T. First-dimension IPG strips were loaded directly onto the slab gels following equilibration for 10 min in Equilibration Buffer I and 10 min in Equilibration Buffer II (Equilibration Buffer I: 6 M urea, 2% SDS, 0.375 M Tris·HCl, pH 8.8, 20% glycerol, 130 mM DTT; Equilibration Buffer II: 6 M urea, 2% SDS, 0.375 M Tris·HCl, pH 8.8, 20% glycerol, 135 mM iodoacetamide). All 20 2-D slab gels were run in parallel at 8°C for 18 h at 160 V and subsequently fixed and stained using a sensitive colloidal Coomassie blue G-250 procedure (7). After 96 h, gels were washed several times with water and scanned at 95.3 μm/pixel resolution using a GS-800 Calibrated Imaging Densitometer (Bio-Rad).

*Image analysis of 2-D gels.* The resulting 12-bit images were analyzed using PDQuest software (v.7.1, Bio-Rad). Background was subtracted, and protein spot density peaks were detected and counted. Because total spot counts and the total optical density are directly related to the total protein concentration, individual protein quantities were thus expressed as parts per million (ppm) of the total integrated optical density, after normalization against total image density. A reference pattern was constructed, and each of the gels in the match set was matched to the reference gel. Numerous proteins that were uniformly expressed in all patterns were used as landmarks to facilitate rapid gel matching. Significant differences in spot intensities among the selected spots were then calculated with a two-sample Student's *t*-test ($P \leq 0.01$). Comparisons were made between pairs of groups with three gels in each group.

Among all 1,000 spots, DCVC altered 439 proteins significantly (≥1.5-fold; $P \leq 0.01$) compared with DW-treated controls. The data indicate that, with DCVC (in *groups II*, *III*, and *IV*), a total of 439 proteins were either increased or decreased (≥1.5-fold change, $P \leq 0.01$) compared with DW-treated controls. With the low dose (15 mg DCVC/kg ip), a total of 30 proteins were found to be modified (9 upregulated; 21 downregulated). With the lethal dose (75 mg DCVC/kg ip), a total of 210 proteins were found to be modified (84 upregulated; 126 downregulated). In autoprotected mice (*group IV*; 15+75 mg DCVC/kg), a total of 199 proteins were found to be modified (91 upregulated; 108 downregulated).

*Liquid chromatography tandem mass spectrometry identification of proteins.* Due to voluminous data produced in these studies, for our first cut we selected those proteins that showed ≥10-fold change, and 18 common proteins fell into this category that were altered in all the groups (*groups I*, *II*, *III*, and *IV*) compared with controls. These 18 proteins were further excised from the gels and minced for their complete sequence identification by liquid chromatography tandem mass spectrometry (LC-MS/MS) techniques. Acrylamide pieces were rinsed with 50 mM ammonium bicarbonate/acetonitrile (1:1, vol/vol), dried, rehydrated in DTT, and alkylated with *N*-isopropyl iodoacetamide (100 mM in 50 mM ammonium bicarbonate). After removal of excess buffer, gel slices were dried, rehydrated in the presence of sequencing grade trypsin, and digested overnight at 37°C. Peptides were eluted using 5% formic acid/50% acetonitrile. Ion spray/nanoelectrospray MS and MS/MS measurements were performed on a Sciex API ± III LC-MS/MS triple-quadrupole instrument (PerkinElmer Biosystems and Sciex). MS results were analyzed using the MassMap (Finnigan) and Peptide-Search (EMBL) programs (54). The XCorr value is the cross-correlation value from the SEQUEST search, an index of confidence in protein identification. The avgXCorr is simply the average of all XCorr scores for multiple peptides from the identified protein (≥2.5 is considered high confidence). This is all calculated in the SEQUEST(tm) software.

*Glucose-regulated protein 75 and proteasome α-subunit type 1 immunohistochemistry.* Formalin-fixed, paraffin-embedded tissues were sectioned at 4 μm and placed onto slides. After being heated at 55°C for 1 h, the sections were deparaffinized in xylene and rehydrated in graded ethanols. Endogenous peroxidase activity was blocked using 3% hydrogen peroxide ($H_2O_2$) in methanol for 10 min. For antigen retrieval, specimens were microwaved in 0.01 mol/l of sodium citrate (pH 6.0) for three changes of 5 min each, followed by cooling in PBS. The sections were incubated in 3% bovine serum albumin made in PBS for 1 h at room temperature. Anti-glucose-regulated protein 75 (GRP75; Sigma) and anti-proteasome α-subunit type 1 (PSA-1; Boston Biochemical, Cambridge, MA) antibodies were applied at a 1:100 dilution, respectively, in 1% bovine serum albumin/PBS and incubated in a humidity chamber at 4°C overnight. After the primary antibody incubation, a secondary horseradish peroxidase linked anti-rabbit antibody (Amersham Pharmacia Biotech, Piscataway, NJ) was applied at a 1:100 dilution (in 1% bovine serum albumin in PBS) for 1 h at room temperature, followed by the application of diaminobenzidine with $H_2O_2$ for 10 min, according to the manufacturer's instructions. The slides were washed in DW and lightly counterstained with hematoxylin. Appropriate negative controls were maintained throughout the experiment.

*Measurement of renal ATP content.* Renal ATP content was evaluated over a time course by luciferase assay using a kit from Sigma-Aldrich according to the manufacturer's instructions. Immediately before the assay was performed, frozen kidney tissue of each mouse (200 mg, stored at −80°C) for each time point ($n = 3$) was homogenized in chilled lysis buffer and centrifuged (13,000 rpm) for 5 min at 4°C. The luciferase activity in the supernatant was evaluated in a Berthold luminometer (Berthold, Bundoora, Australia). ATP content in the samples was determined by comparison to a concurrently determined standard curve, and the results are expressed as micromoles ATP per gram kidney.

*Data and statistical analysis.* Data [plasma creatinine concentration, ATP concentration, and quantitative assessment (fold-change) of the differential expression of proteins] were expressed as means ± SE ($n = 3$) for all the experiments. Comparison between different time points for each group was determined by one-way analysis of variance followed by Tukey's honestly significantly different and Duncan's multiple range tests using SPSS (SPSS, Chicago, IL). For image analysis, the statistical significance of differences in fold-changes between control and treatment groups at the same time point was analyzed by Student's *t*-test. In all cases, $P \leq 0.01$ was used to determine statistically significant differences.

## RESULTS

*Lethality study.* To confirm and reproduce our earlier findings, a separate lethality study was conducted with a new set of mice. As observed and reported previously (27, 28, 64–66), 90% of the mice receiving the high dose of DCVC (75 mg/kg) died between 36 and 48 h after dosing (28, 64, 65). When a priming low dose of DCVC (15 mg/kg) was given 72 h before the administration of a normally lethal dose of DCVC (75 mg/kg), all the mice survived (Table 1). Renal failure and mortality observed in the unprimed high-dose-treated mice were comparable to the results of our previous studies (28). Mice given DW alone showed no signs of morbidity or mortality at any time point.

*Renal function.* With the low dose (15 mg DCVC/kg), renal function was decreased as evidenced by plasma creatinine elevation at 36 h after dosing and then returned to normal by 72 h (Fig. 1*A*). With the high dose, mice experienced marked and progressive renal failure, as assessed by significant elevations in creatinine through 24–36 h (96–108 h in Fig. 1*B*) after 75 mg DCVC/kg. Administration of distilled water used as the vehicle for DCVC did not alter renal function (Fig. 1B). In the autoprotected mice, renal function was compromised, as evidenced by significant elevation in plasma creatinine at 24 and 36 h after the administration of a high dose of DCVC (96 and 108 h after a low dose, Fig. 1*C*). However, these levels were significantly lower compared with the high dose alone at the same time points (Fig. 1*B*). Renal function recuperates as early as 144 h (3 days after the high dose in Fig. 1*C*), as evidenced by low basal levels of plasma creatinine from this time point onward.

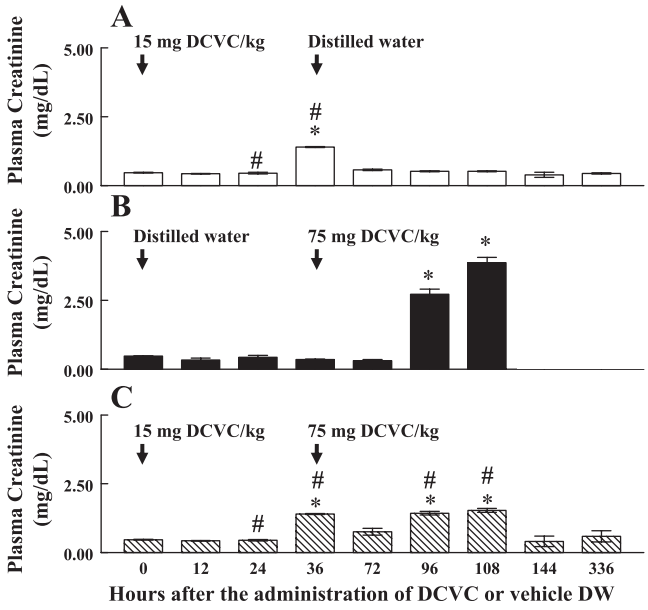


Fig. 1. Time course of plasma creatinine levels following *S*-(1, 2-dichlorovinyl)-L-cysteine (DCVC) administration in low-dose, high-dose, and low-dose followed 3 days later by high-dose-treated mice. *A*: In the low-dose group, male Swiss Webster (SW) mice ($n = 3$) were injected with a single dose of DCVC (15 mg/kg ip) in distilled water (DW; 10 ml/kg) at 0 h followed by a single administration of DW (10 ml/kg ip) 72 h after DCVC administration. *B*: in the high-dose group, male SW mice ($n = 3$) were injected with DW (10 ml/kg ip) at 0 h followed by DCVC (75 mg/kg ip) in DW (10 ml/kg) 72 h after the exposure to DW at 0 h. *C*: in the autoprotected group, male SW mice ($n = 3$) were injected with DCVC (15 mg/kg ip) in DW (10 ml/kg) at 0 h followed by DCVC (75 mg/kg ip) in DW (10 ml/kg) 72 h after the administration of low dose. Arrows indicate the time of administration of respective doses of DCVC or DW vehicle at time points 0 and 72 h. Values are means ± SE ($n = 3$). *Statistically higher than respective 0 h controls. #Statistically lower than 75 mg DCVC/kg at that particular time point. $P \leq 0.01$.

*Renal injury.* Kidney injury was examined by hematoxylin- and eosin-stained light microscopic examination of the renal sections from mice in all groups. Histological examination of kidneys in mice treated with a low dose confirmed mild renal proximal tubular necrosis compared with controls at the 36-h time point (* in Fig. 2*B*). This injury regressed at later time points, and mice recovered completely from DCVC-initiated renal damage. As expected, in mice that received a high dose, extensive proximal tubular necrosis was evident 36 h after dosing (108 h after DW treatment). This was characterized by amorphous, intensely eosinophilic tubules with ghostly silhouettes of karyolitic nuclei (# in Fig. 2*C*), and the injury then progressed through 108 h, damaging almost the entire CMR (Fig. 2*C*) of the kidney. At later time points, the injury progressed to affect the inner medullary and outer cortical regions, resulting in 90% mortality by 36–48 h after the high dose (Table 1). There was minimal to no evidence of proximal tubule repair 36 h after 75 mg DCVC/kg (Fig. 2*C*). In the autoprotected mice, there was clear evidence of renal tubular repair characterized by marked renal tubule basophilia and squamous to low cuboidal reepithelialization inside residual tubular basal lamina at 36 h (108 h after the low-dose treatment, @ in Fig. 2*D*). This led to recovery from renal injury, and the mice survived (Table 1).

*Proteomic analysis of DCVC-induced renal damage in male SW mice.* The effects of low, high, and combination doses of DCVC on the expression of mouse kidney proteins at 36 h after respective treatments were assessed by 2-DE analysis of tissues ($n = 3$ mice/group) (Fig. 3). Verification of renal injury was available at 36 h after respective treatments in the low-dose, high-dose, and autoprotected groups by histopathology. Cellular proteins recovered and displayed were distributed across the isoelectric point (pI) range 4.5–9.0, with molecular masses between 10,000 and 80,000 Da. To identify changes in protein expression between the different groups, the gels were analyzed using PDQuest software (Bio-Rad). Approximately 1,000 proteins were detected, among which 439 proteins were found to be differentially expressed among all the groups (data not shown). Densitometric analysis of these 439 protein spots in low-dose, high-dose, and autoprotected mice revealed statistically significant differential expression compared with controls (by 1.5-fold or more at $P \leq 0.01$). Of these 439 proteins, with a low dose (15 mg DCVC/kg ip) a total of 30 proteins were found to be modified (9 upregulated; 21 downregulated). With a lethal dose (75 mg DCVC/kg ip), a total of 210 proteins were found to be modified (84 upregulated; 126 downregulated). In autoprotected mice (15+75 mg DCVC/kg), a total of 199 proteins were found to be modified (91 upregulated; 108 downregulated). Due to the large amount of data produced in these studies, we selected those proteins (18 proteins) that were maximally altered (≥10-fold) commonly in all the groups (*groups II*, *III*, and *IV*) by DCVC treatment compared with controls (*group I*). These 18 proteins were unambiguously identified with high scores and categorized functionally as stress response and protein repair chaperones: GRP75/mortalin/heat shock protein (HSP) 74 (2942), stress-

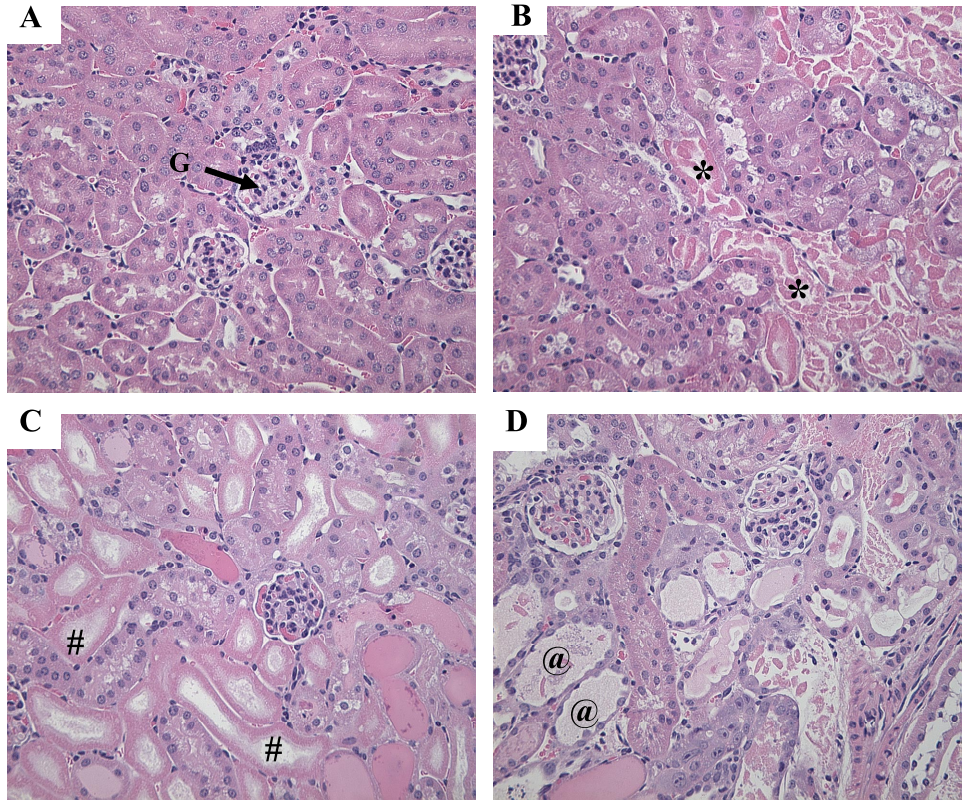


Fig. 2. Representative photomicrographs of hematoxylin- and eosin-stained kidney sections isolated from mice at 36 h after respective treatments: *A*: mice in *group I* treated with DW (10 ml/kg) alone showed no necrosis at 36 h. *B*: mice in *group II* treated with 15 mg DCVC/kg show minimal necrosis (*) in proximal tubules at 36 h. *C*: mice in *group III* treated with 75 mg DCVC/kg showed extensive and significant renal damage characterized by intensely eosinophilic and necrotic proximal tubular epithelium with some exfoliation of cellular detritus into tubular lumens (#) at 36 h. *D*: mice in *group IV*, after pretreatment with 15 mg DCVC/kg, received 75 mg DCVC/kg at 72 h (autoprotection protocol). Despite extensive renal damage, robust tubular repair was also evident, characterized by squamous to low cuboidal reepithelialization of tubules (@) with typical cytoplasmic basophilia and slight karyomegally of the newly regenerated epithelium at 36 h after the high dose (108 h after the priming dose). All fields were chosen from the corticomedullary region (CMR) encompassing the outer stripe of the outer medulla (OSOM). G, glomerulus. Original magnification, ×200.

induced phosphoprotein (5812), and hemopexin (Hx; 3925); proteins involved in the elimination of glyoxal-related toxic byproducts: glyoxalase domain containing 4 (Glod4; *Mus musculus*) (1414); transporters: very-long-chain acyl-CoA sythetase/fatty acid transporter-2 (FATP-2; 3008); participants in protein turnover: PSA-1 (4407); translational factors: translation elongation factor (5702); free radical scavengers: peroxiredoxin-5 (PRDX5; 8151); and proteins involved in maintaining cellular energetics and ATP levels: inorganic pyrophosphatase-2 (3527), lactate dehydrogenase (LDH; 3706), 3-hydroxyanthranilate 3,4-dioxygenase isoform 1 (4418), α-enolase (ENOA; 4728), short-chain acyl-CoA dehydrogenase (ACADS; 5604), sorbitol dehydrogenase (DHSO; 5621), alcohol dehydrogenase $NADP^+$ (AK1A1; 6514), acetyl-CoA acetyltransferase 1 (7620), pyruvate kinase isozyme M2 (KPYM, 7843), and malate dehydrogenase (MDH; 8513). The identities of all of these 18 proteins and their biochemical properties/functions are listed in Tables 2 and 3, respectively.

*Proteomic analysis of DCVC-induced stress response: GRP75/mortalin/HSP 74, hemopexin precursor, stress-induced phosphoprotein, and Glod4 (Mus musculus).* In general, DCVC treatment caused downregulation of GRP75 protein expression compared with the DW-treated controls (Table 3). GRP75 was slightly downregulated (2.8 ± 0.11-fold) with a low dose of DCVC compared with controls. With a high dose of DCVC, GRP75 was substantially downregulated (55 ± 17.8-fold) compared with controls (Table 3). Quite remarkably, when the low dose-primed mice were challenged with the high dose, GRP75 was only moderately downregulated [with low dose + high dose, 9.5 ± 3.9 compared with high dose, 55 ± 17.8 (Table 3)]. These findings are consistent with GRP75 immunohistochemical staining in the CMR in the kidney sections (Fig. 4). GRP75 was expressed in the inner stripe of the outer medulla also apart from the regions of damage in S3 segments of the CMR encompassing the outer stripe of the outer medulla (OSOM) during the course of renal injury and repair. This expression extends into the inner medulla (data not shown). However, GRP75 expression was evident only in the regions of the OSOM which are the primary targets for DCVC. Cytoplasmic localization of GRP75 at 24, 36, and 72 h after the low dose (Fig. 4, *B–D*) was slightly less compared with normal constitutive levels in 0 h control mice (Fig. 4*A*). With the high dose alone, GRP75 severely progressively declined at 24 and 36 h after the high-dose administration (Fig. 4, *E* and *F*). This finding is evidenced by the lack of GRP75-positive staining in the proximal convoluted tubular epithelial cells in the CMR surrounding the OSOM (Fig. 4, *E* and *F*). In contrast, in the autoprotected mice, higher cytoplasmic expression of GRP75 in tubular epithelial cells was observed at 24 (96 h after the low dose), 36 (108 h after the low dose), and 72 h (144 h after the low dose), respectively, after the high dose (arrows in Fig. 4, *G–I*) compared with lethal dose alone group.

Stress-induced phosphoprotein was found to be downregulated slightly in the low-dose and autoprotected groups, whereas in the high-dose group it is markedly downregulated (Table 3). Hemopexin precursor is a 60-kDa plasma glycoprotein which belongs to the family of the acute-phase proteins whose synthesis may be induced by several cytokines as a result of inflammatory processes. The differences in the upregulation of hemopexin between the low- and high-dose groups were not statistically different. However,

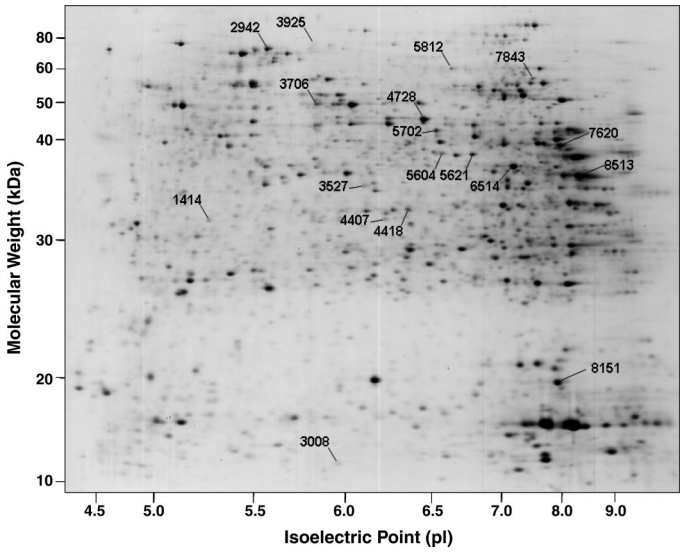


Fig. 3. Representative Coomassie blue-stained two-dimensional gel electrophoresis (2-DE) pattern of male SW mouse kidney homogenate showing resolution of separated proteins 36 h after DCVC in respective treatment groups. Treatment details are described below. The pH range (4.5–9.0) is from *left* to *right* on the *x*-axis, and the molecular weight is from *top* to *bottom* on the *y*-axis. Master spot number (MSN) of 18 proteins whose abundance was significantly altered by DCVC in the respective treatment groups (*A-D* described below) compared with DW controls ($P \leq 0.01$) are depicted. Proteins with MSN 1414, 2942, 3008, 3527, 3706, 3925, 4407, 4418, 4428, 5604, 5621, 5702, 5812, 6514, 7620, 7843, 8151, and 8513 were detected in all the gels, and comparisons were made between controls and respective treatment groups. Data were analyzed using PDQuest image analysis software. Groupwise statistical comparisons were made by Student's *t*-test to screen for protein alterations. These 18 protein spots that were altered differentially were tryptically digested, yielding masses subjected to liquid chromatography tandem mass spectrometry for protein identification. Quantitative and qualitative differences were analyzed statistically and are listed in Tables 2 and 3. *A*: in controls, kidneys were collected from mice 36 h after the initial treatment, and whole-kidney homogenates were made in the lysis buffer. To run 2-DE, 500 μg protein/gel ($n = 3$ gels) were used. *B*: in the low-dose (LD) group, kidneys were collected from mice 36 h after the initial treatment, and whole-kidney homogenates were made in the lysis buffer. To run 2-DE, 500 μg protein/gel ($n = 3$ gels) were used. *C*: in the high-dose (HD) group, kidneys were collected from mice 108 h after the initial treatment (36 h after the high dose), and whole-kidney homogenates were made in the lysis buffer. To run 2-DE, 500 μg protein/gel ($n = 3$ gels) were used. *D*: in the autoprotected group (LD+HD), kidneys were collected from mice 108 h after the initial treatment (36 h after the high dose), and whole-kidney homogenates were made in the lysis buffer. To run 2-DE, 500 μg protein/gel ($n = 3$ gels) were used.

in the autoprotected mice, the overexpression of hemopexin was significantly higher compared with low/high-dose groups (Table 3). With the low dose, Glod4 protein was mildly suppressed (1.4 ± 0.2 fold) compared with the controls. In contrast, with the lethal dose alone, it was markedly downregulated (37.5 ± 19.6-fold) compared with the controls (Table 3). Interestingly, if the mice were primed with a low dose, this protein is only moderately downregulated (3 ± 0.26-fold) after the high-dose challenge.

*Proteins involved in fatty acid transport: very-long-chain acyl-CoA synthetase or FATP-2.* Image analysis of this protein in our 2-DE experiments revealed that this protein was downregulated significantly following a lethal dose of DCVC (Table 3). In contrast, in the low-dose and autoprotected groups, FATP-2 was only modestly downregulated compared with the controls (Table 3).

*Proteins involved in protein turnover, translation elongation, and free radical scavenging: PSA-1, translation elongation factor, and PRDX5.* In our proteomics findings, with a low dose of DCVC, PSA-1 was upregulated moderately. In contrast, with a high dose, its expression was suppressed ~11-fold compared with the controls. However, in the autoprotected mice, its downregulation was very minor compared with the high dose of DCVC alone (Table 3). These findings were confirmed by PSA-1 immunohistochemical staining in the CMR in the kidney sections (Fig. 5). PSA-1 was expressed in the inner stripe of the outer medulla also apart from the regions of damage in S3 segments of the CMR encompassing the OSOM during the course of renal injury and repair. The expression of this protein extends into the inner medulla (data not shown). However, PSA-1 localization was evident only in the regions of the OSOM, which is the primary target for DCVC. Cytoplasmic localization of PSA-1 at 24, 36, and 72 h after the low dose (Fig. 5, *B–D*) was slightly higher compared with normal constitutive levels at 0 h in the control mice (Fig. 5*A*). This expression extends into the inner medulla (data not shown). With the high dose alone, PSA-1 was severely and progressively downregulated at 24 and 36 h after the high-dose administration (Fig. 5, *E* and *F*). This finding is evidenced by lack of PSA-1-positive staining in the proximal convoluted tubular epithelial cells in the CMR surrounding the OSOM (Fig. 5, *E* and *F*). By contrast, in the autoprotected mice higher cytoplasmic expression of PSA-1 was observed in tubular epithelial cells at 24 (96 h after the low dose), 36 (108 h after the low dose), and 72 h (144 h after the low dose), respectively, after the high dose (arrows in Fig. 5, *G–I*) compared with lethal dose alone group.

In the low-dose and autoprotected groups, translation elongation factor was moderately downregulated, whereas with a lethal dose alone it was substantially underexpressed (Table 3), suggesting inhibition of essential protein synthesis necessary for cell division and repair following injury. PRDX5 was suggested to play a role in preventing the development of oxidative damage (58). Proteomic findings in the present study revealed that with high dose alone PRDX5 was downregulated substantially compared with the autoprotected mice. In contrast, after the low dose PRDX5 was slightly upregulated compared with controls (Table 3).

*DCVC-induced changes in cellular energetics.* Various mitochondrial precursor proteins involved in cellular respiration and ATP production are downregulated severely by the lethal dose of DCVC alone (Table 3). In contrast, in low-dose and autoprotected groups, after DCVC the downregulation of these proteins was mild to moderate (Table 3). We measured renal ATP content in mice over a time course after the administration of DCVC, at low dose, high dose, and in autoprotected mice (Fig. 6). Severe depletion of ATP was evident at 6–36 h after the high dose of DCVC (Fig. 6*B*). After the low dose of DCVC, renal ATP levels were maintained for 36 h, albeit with a slight but insignificant decline after dosing before dramatically declining to the lowest level by 72 h (Fig. 6*A*). This decline is due to utilization of energy to support replicative DNA synthesis that peaks at 72 h (63, 64) needed for tissue repair and recovery (27, 28, 63, 64). ATP content then recovered completely after an additional 36 h (108 h in Fig. 6*A*), and this paralleled restoration of kidney structure and function (Fig. 6*A*). Restoration of normal ATP levels would be expected after

Table 2. *Summary of LC-MS/MS data obtained from male SW mouse total kidney homogenate protein spots altered by DCVC*

| Identity (SwissProt Identifier) [MSN] | Molecular Mass, kDa | ID No. | pI | avgXCorr | No. of Identified Peptides |
|---|---|---|---|---|---|
| Stress-70 protein, mitochondrial prec.(GRP75_mouse) [2942] | 73.528 | P38647 | 5.91 | 3.43 | 30 |
| Stress-induced phosphoprotein-1 [5812] | 65.728 | Np058017 | 6.50 | 2.70 | 13 |
| Hemopexin prec. (Hemo_mouse) [3925] | 51.341 | Q91X72 | 7.92 | 2.72 | 2 |
| Glyoxalase domain-containing protein 4 [1414] | 33.317 | Np080305 | 5.30 | 3.66 | 10 |
| Very-long-chain acyl-CoA synthetase (FATP-2_mouse) [3008] | 70.366 | O35488 | 9.02 | 3.41 | 10 |
| Proteasome subunit-α type 1 (PSA1_mouse) [4407] | 29.547 | Q9R1P4 | 6.00 | 2.56 | 8 |
| Translation elongation factor, mitochondrial [5702] | 49.508 | Np766333 | 6.7 | 3.52 | 38 |
| Peroxiredoxin-5, mitochondrial prec. (PRDX5_mouse) [8151] | 21.897 | P99029 | 9.10 | 3.10 | 9 |
| Inorganic pyrophosphatase-2_mouse [3527] | 38.115 | Np666253 | 6.10 | 3.69 | 14 |
| D-Lactate dehydrogenase (LDH_mouse) [3706] | 51.848 | Np081846 | 5.8 | 3.44 | 14 |
| 3-Hydroxyanthranilate 3,4-dioxygenase isoform 1_mouse [4418] | 32.902 | Xp354652 | 6.3 | 2.72 | 11 |
| α-enolase (ENOA_mouse) [4728] | 47.125 | P17182 | 6.36 | 3.42 | 50 |
| Acyl-CoA dehydrogenase, short-chain specific, mitochondrial prec. (ACADS_mouse) [5604] | 44.947 | Q07417 | 6.5 | 3.39 | 7 |
| Sorbitol dehydrogenase (DHSO_mouse) [5621] | 40.091 | Q64442 | 6.60 | 3.93 | 33 |
| Alcohol dehydrogenase $NADP^+$ (AK1A1_mouse) [6514] | 36.456 | Q9JII6 | 6.87 | 3.17 | 44 |
| Acetyl-Coenzyme A acetyltransferase 1 prec_mouse [7620] | 44.816 | Np659033 | 7.8 | 3.07 | 30 |
| Pyruvate kinase isozyme M2 (KPYM_mouse) [7843] | 57.948 | P52480 | 7.42 | 3.53 | 28 |
| Malate Dehydrogenase (MDH_mouse) [8513] | 31.081 | Xp354795 | 8.5 | 3.59 | 20 |

LC-MS/MS, liquid chromatography tandem mass spectrometry; MSN, master spot number depicted on the gel; ID no, protein accession ID number to search for the protein for protein information in SwissProt/EMBL international protein identification database; pI, isoelectric point of proteins; avgXCorr, average cross correlation as an index of confidence in protein identification (≥2.5 is considered high confidence); prec., precursor. See METHODS for details.

the replacement of lost cells with functional cells. Similarly, in the autoprotected mice, ATP content declined exactly as in the low dose alone group before recovering to normal levels after an additional 72 h after the high dose of DCVC (144 h after low dose, Fig. 6*C*), in stark contrast to the high dose alone-treated mice (Fig. 6*B*). After the high dose alone, while ATP is utilized for cellular defenses and for stimulation of unsuccessful cell division, restoration of ATP does not occur due to the lack of new cells.

## DISCUSSION

Nephro-autoprotection is defined as renal protection offered by prior administration of a low dose of DCVC to mice followed by subsequent administration of a normally lethal high dose of DCVC (65). Protection is due to prompt upregulation of compensatory cell division signaling mechanisms and proximal tubular epithelial repair which mitigate the progression of renal injury, allowing the mice to recover from ARF-bound injury from the high dose and animal death (27, 28, 64–66). The objective of the present study was to identify renal protein changes following DCVC-induced ARF and their role in recovery from ARF-bound injury and death in the autoprotected mice. This is the first report demonstrating dose-related differential protein expression patterns following DCVC-induced ARF in mice.

We used 2-DE and LC-MS/MS to identify proteins that were differentially expressed following renal proximal tubular cell damage and ARF-bound injury initiated by the nephrotoxic cysteine conjugate DCVC in mice. We used a proteomic approach to track the key proteins that closely correspond with recovery from DCVC-initiated renal injury in the autoprotection model. We identified and functionally categorized 18 different proteins that were changed (≥10-fold) by DCVC into the following categories: cellular stress response proteins; glyoxal elimination; fatty acid transport; protein repair and turnover; translation elongation factor; free radical scavenging; and cellular energetics. Our study illustrates the power of proteomics in understanding how specific pathways of injury or recovery from injury are affected by the severity of ARF. It also illustrates that new insights may be obtained into protection against progression of renal injury mediated by expression of functional proteins.

*Role of stress response proteins in DCVC-induced renal damage and recovery.* High metabolic activity of proximal tubular epithelial cells in the S3 segments make them particularly vulnerable targets of necrotic or apoptotic effects of ischemia and nephrotoxicants. DCVC-induced cellular damage leads to prominent changes in stress response proteins (15). GRP75/HSP74 has multiple functions ranging from stress responses to intracellular trafficking, antigen processing, control of cell proliferation, and differentiation (5, 25, 32, 45, 71–73). After injury, GRP75/mortalin/HSP74, an important molecular chaperone of the HSP70 family (19, 35, 60), facilitates the restoration of normal function by assisting in the refolding of denatured proteins, degradation of irreparably damaged proteins and toxic metabolites, aggregation of damaged peptides, and by aiding appropriate folding of newly synthesized essential polypeptides (60). HSP90 is known to aid in the regeneration of damaged cells in the S3 segment of proximal tubules, during the course of cisplatin-induced acute tubular injury (49). HSPs (HSP25/72) are known to protect against ischemia-induced injury in the kidney (9, 16, 26, 51, 57, 68). Recently, HSP27 has been shown to be involved in the renal epithelial ($LLC\text{-}PK_1$) cellular stress response following DCVC exposure (15). This finding is consistent with earlier observations with HSP25 and HSP72, where it was shown that renal ischemic preconditioning in mice increased the expression of HSPs (HSP25/72), offering protection against subsequent ischemia-reperfusion injury and ARF (26). Therefore, with low-dose priming, GRP75/HSP74 might not be allowing the high dose-induced cellular injury to progress either via primary induction of cytoresistance or by simultaneous en-

Table 3. *Summary of fold-change differences and functional categories of identified proteins altered by DCVC in male SW mouse whole kidney homogenates*

| Identity (SwissProt identifier) [MSN] | Fold-Difference (±SE) Compared With DW Controls | | |
|---|---|---|---|
| | LD | HD | LD+HD (Autopr.) |
| Stress response, protein repair participants, and antioxidants | | | |
| Stress-70 protein, mitochondrial prec. (GRP75_mouse) [2942] | −2.8 (±0.11) | −55 (±17.8) | −9.5 (±3.9) |
| Stress-induced phosphoprotein-1 [5812] | −1.4 (±0.06) | −12.8 (±3.5) | −2.2 (±0.3) |
| Hemopexin prec. (Hemo_mouse) [3925] | 4.2 (±2.2) | 24.5 (±21) | 45 (±31) |
| Glyoxalase domain-containing protein 4 [1414] | −1.4 (±0.2) | −37.5 (±19.6) | −3 (±0.26) |
| Fatty acid transporter | | | |
| Very-long-chain acyl-CoA synthetase (FATP-2_mouse) [3008] | 1.8 (±0.1) | −10.6 (±6.7) | –3 (±0.4) |
| Protein turnover | | | |
| Proteasome subunit-α type 1 (PSA1_mouse) [4407] | 0.98 (±0.08) | –11 (±5.3) | –2 (±0.2) |
| Translation, elongation factor | | | |
| Translation elongation factor, mitochondrial [5702] | −1.3 (±0.3) | −13 (±6.8) | −3.26 (±0.3) |
| Scavengers of oxygen radicals | | | |
| Peroxiredoxin-5, mitochondrial prec. (PRDX5_mouse) [8151] | 1.2 (±0.3) | −16.3 (±5.8) | −3.9 (±1) |
| Energy metabolism | | | |
| Inorganic pyrophosphatase-2_mouse [3527] | −1.9 (±0.11) | −27 (±7.1) | −8.4 (±1.5) |
| D-lactate dehydrogenase (LDH_mouse) [3706] | −2.4 (±1.0) | −10.6 (±5.5) | −2.4 (±0.6) |
| 3-Hydroxyanthranilate 3,4-dioxygenase isoform 1_mouse [4418] | −1.6 (±0.2) | −36.5 (±12.9) | −11 (±0.3) |
| α-Enolase (ENOA_mouse) [4728] | −1.3 (±0.14) | −27.7 (±20) | −2.3 (±0.18) |
| Acyl-CoA dehydrogenase, short-chain specific, mitochondrial prec. (ACADS_mouse) [5604] | −1.9 (±0.3) | −50 (±18.9) | −10.7 (±0.8) |
| Sorbitol dehydrogenase (DHSO_mouse) [5621] | −1.7 (±0.3) | −21.4 (±1.34) | −6.7 (±0.3) |
| Alcohol dehydrogenase $NADP^+$ (AK1A1_mouse) [6514] | −1.3 (±0.14) | −33 (±21.1) | −5.3 (±0.6) |
| Acetyl-CoA acetyltransferase 1 prec_mouse [7620] | −2 (±0.5) | −19.8 (±2.8) | −13.8 (±0.6) |
| Pyruvate kinase isozyme M2 (KPYM_mouse) [7843] | −1.3 (±0.2) | −14 (±5.4) | −1.7 (±0.15) |
| Malate dehydrogenase (MDH_mouse) [8513] | −1.5 (±0.5) | −31 (±13.7) | −3.8 (±1.1) |

In the low-dose (LD) group, male SW mice ($n = 3$) were injected with a single dose of DCVC (15 mg/kg ip) in DW (10 ml/kg) at 0 h, and kidneys were removed at 36 h after LD of DCVC and total homogenates were made. In the high-dose (HD) group, male SW mice ($n = 3$) were injected with DW (10 ml/kg ip) at 0 h followed by DCVC (75 mg/kg ip) in DW (10 ml/kg) 72 h after the exposure to DW at 0 h. Mice start dying from 36 h onward after the lethal dose administration (108 h onward after DW). Kidneys were removed at 36 h after the HD of DCVC, and total homogenates were made. In the autoprotected (Autopr.) group, male SW mice ($n = 3$) were injected with DCVC (15 mg/kg ip) in DW (10 ml/kg) at 0 h followed by DCVC (75 mg/kg ip) in DW (10 ml/kg) 72 h after the administration of the low dose. Kidneys were removed from the mice at 36 h after the high dose (108 h after low dose), and whole kidney homogenates were made for proteomic studies and identification of proteins by LC-MS/MS.

hancement of cellular repair and recovery mechanisms in the autoprotected mice. This is corroborated by renal histopathology of kidney sections taken from mice in low-dose, high-dose, and autoprotected groups (Fig. 2). The mechanism by which HSP74 prevents progression of DCVC-induced injury is unknown. However, taking together the evidence on the cytoprotective role of other HSPs from the literature and from the present findings, it may be suggested that GRP75/HSP74 is closely linked with cytoprotection. With the high dose alone, DCVC-induced stress is so intense that GRP75/HSP74 is severely downregulated and cell death is inevitable. However, exposure of cells to mild low-dose DCVC-induced stress is sufficient to induce the expression and accumulation of GRP75/HSP74, which protects against a subsequent challenge from high dose-induced stress in the autoprotected mice. This is evident by only moderate downregulation of GRP75/HSP74 after the high dose in autoprotected mice compared with severe downregulation observed in nonprimed mice challenged with high dose alone. Therefore, GRP75/HSP74 might be involved in survival of the damaged cells, and the next investigative challenge will be to define the regulatory pathways of the GRP75/HSP74 cellular stress response in DCVC-induced autoprotection and ARF. Due to large amounts of data produced by these studies, only the maximally altered 18 proteins (≥10-fold by DCVC treatment) commonly in all the groups (low-dose, high-dose, and autoprotected) were identified by LC/MS/MS. To avoid cost and time constraints in this study, proteins that are maximally altered were prioritized for identification. Therefore, as of now there is a dearth of information about other HSPs with regard to whether they were altered during DCVC-induced necrosis. However, it is anticipated that there will be significant changes in other HSPs after DCVC treatment.

Stress-induced phosphoprotein-1 was shown to interact with Hsp70 and Hsp90 and facilitates transfer of substrates from Hsp70 to Hsp90 and is important for proper protein folding, maturation, and cell cycle progression (8, 22, 36, 67). We propose that severe downregulation of stress-induced phosphoprotein-1 with high dose alone might have disturbed the key interaction between stress-induced phosphoprotein-1 and various HSPs, leading to cell death, compared with sustained expression of stress-induced phosphoprotein-1 and activation of survival pathways in autoprotected mice. Hemopexin is a 60-kDa plasma glycoprotein member of the acute-phase protein family, whose synthesis may be induced by several cytokines during inflammation (3, 43). Hemopexin is involved in various biochemical processes: protection of renal tubules against hemoglobin-mediated oxidative damage (62); induction of heme oxygenase 1 (HO-1), ferritin, and metallothionein 1 (MT-1) genes that function as antioxidants (2, 56); and activation of JNK/SAPK and nuclear translocation of NF-κB (17). In the autoprotected mice, the overexpression of hemopexin was significant compared with the low- and high-dose

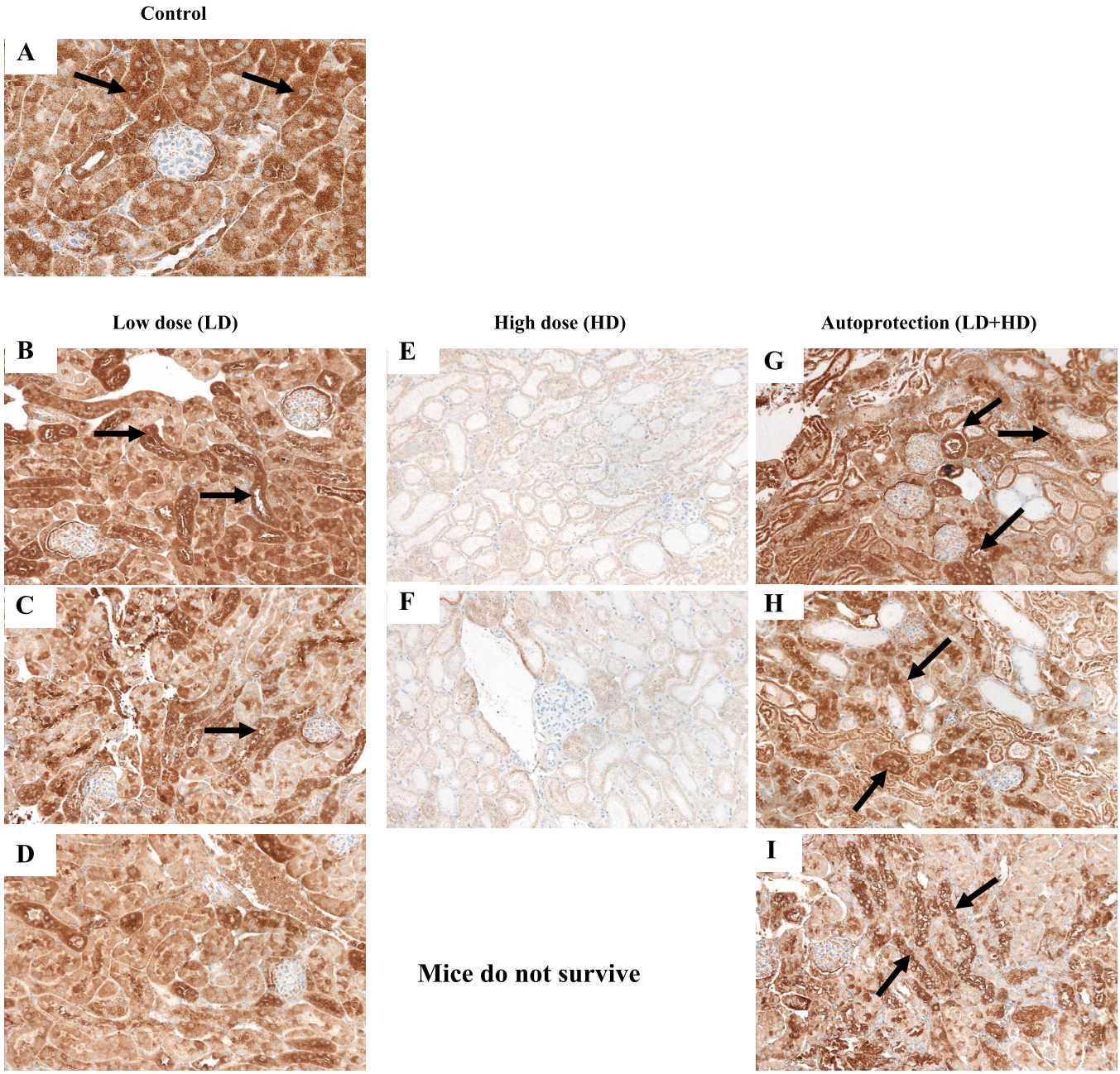


Fig. 4. Representative photomicrographs of glucose-regulated protein 75 (GRP75) immunohistochemistry of kidney sections. *A*: in the control group, mice in *group I* treated with DW (10 ml/kg) alone showed significantly higher constitutive levels of GRP75 at 0 h. In the LD group, mice in *group II* treated with 15 mg DCVC/kg show cytoplasmic staining for GRP75 in the proximal tubular epithelial cells (arrowheads) at 24 (*B*), 36 h (*C*), and 72 h (*D*) after the low dose. In the HD group, mice in *group III* treated with 75 mg DCVC/kg showed significantly lower staining for GRP75 in the proximal tubular epithelium at 24 (*E*) and 36 h (*F*) after the high dose. In the LD + HD group, mice in *group IV*, after pretreatment with 15 mg DCVC/kg, received 75 mg DCVC/kg at 72 h (autoprotection protocol). Significantly higher cytoplasmic expression of GRP75 in tubular epithelial cells (arrows) was evident at 24 (96 h after the low dose; *G*), 36 (108 h after the low dose; *H*), and 72 h (144 h after the low dose; *I*), respectively, after the high dose in autoprotected mice compared with lethal dose alone group. All fields were chosen from the CMR encompassing the OSOM. Original magnification, ×200.

groups (Table 3), bringing to bear all the protective effects of hemopexin in the autoprotected kidney.

DCVC and/or its metabolites are known to kill renal epithelial cells by a combination of covalent binding, depletion of nonprotein thiols, and lipid peroxidation (4, 10, 21). DCVC-induced lipid peroxidation leads to formation of various harmful physiological metabolites like glyoxal and methylglyoxal (MG) that are known to induce oxidative stress, protein glycation, and eventual cell death (53). Glyoxal and MG are detoxified by cytosolic glyoxalase system (glyoxalase I and II) to form glyoxal to glycolate and MG to D-lactate, respectively (61). The coupled reaction catalyzed by the glyoxalase system converts the electrophilic cytotoxic 2-oxoaldehydes to less reactive chemical species. Due to this, the glyoxalases are considered as part of GSH-dependent detoxifying enzymes (12). In our study, we found that Glod4 protein was severely

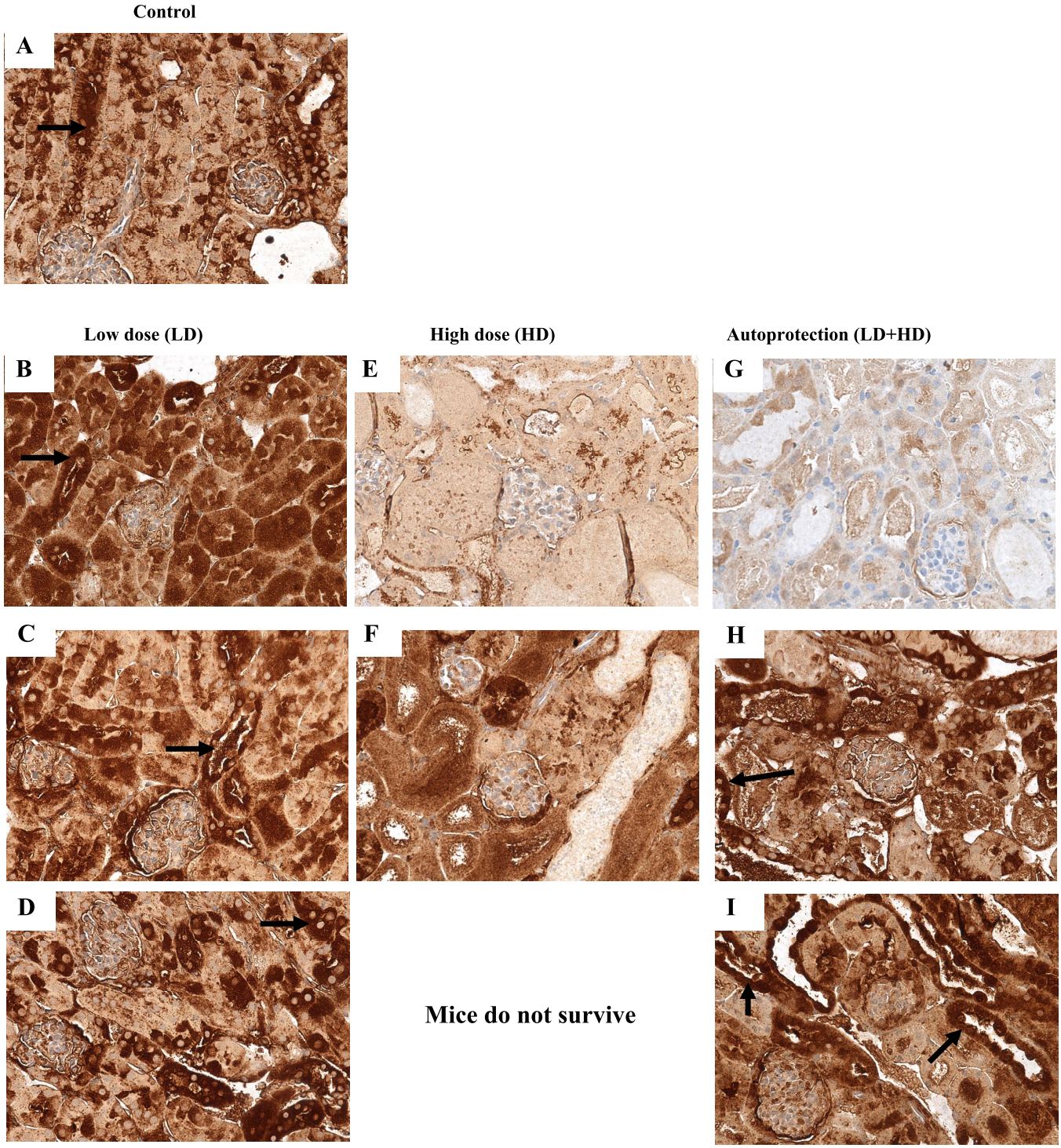


Fig. 5. Representative photomicrographs of proteasome α-subunit type 1 (PSA-1) immunohistochemistry of kidney sections. *A*: in the control group, mice in *group I* treated with DW alone (10 ml/kg) showed constitutive levels of PSA-1 at 0 h. In the LD group, mice in *group II* treated with 15 mg DCVC/kg show cytoplasmic staining for PSA-1 in the proximal tubular epithelial cells (arrowheads) at 24 (*B*), 36 (*C*), and 72 h (*D*) after the low dose. In the HD group, mice in *group III* treated with 75 mg DCVC/kg showed significantly lower staining for PSA-1 in the proximal tubular epithelium at 24 (*E*) and 36 h (*F*) after the high dose. In the LD + HD group, mice in *group IV*, after pretreatment with 15 mg DCVC/kg, received 75 mg DCVC/kg at 72 h (autoprotection protocol). PSA-1 was not that prominent at 24 h (96 h after the low dose; *G*) after the high-dose administration in autoprotected mice. Substantially higher cytoplasmic expression of PSA-1 in tubular epithelial cells (arrows) was evident at 36 (108 h after the low dose; *H*) and 72 h (144 h after the low dose; *I*) after the high dose in autoprotected mice compared with lethal dose alone group. All fields were chosen from the CMR encompassing the OSOM. Original magnification, ×400.

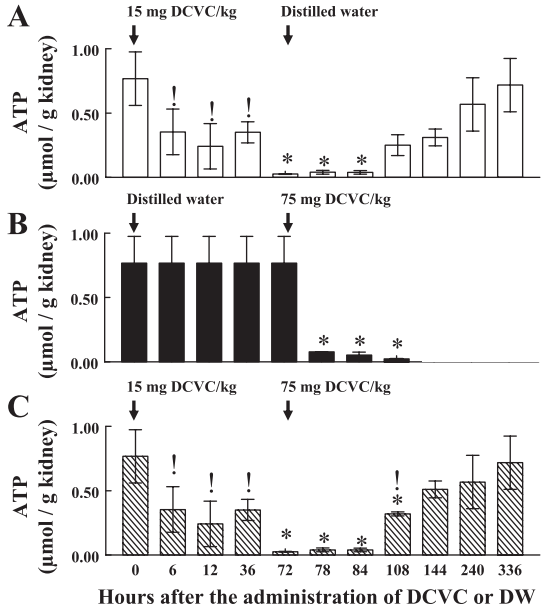


Fig. 6. ATP levels measured in the whole kidney homogenates in LD, HD, and LD + HD groups. *A*: LD group. ATP levels were measured until 336 h after the low dose. *B*: HD group. ATP levels were measured until 36 h after the high dose alone (108 h after DW). Mice start dying from 36 h onward after the lethal dose administration precluding measurement of ATP content. *C*: LD + HD group. ATP levels were measured until 336 h after the priming dose (264 h after the high dose). Arrows indicate the time of administration of respective doses of DCVC or DW vehicle at 0- and 72-h time points. Values are means ± SE ($n = 3$). *Statistically lower than respective 0-h control. ‡Statistically higher than 75 mg DCVC/kg at that particular time point. $P \leq 0.01$.

downregulated (37.5 ± 19.6) after the high dose compared with the mice primed with a low dose of DCVC in the autoprotected group (3 ± 0.26-fold) (Table 3). As a consequence, severe downregulation of the glyoxalase system after the high dose of DCVC might fail to prevent the accumulation of toxic by-products of DCVC-induced lipid peroxidation, eventually leading to oxidative damage and compromised cell viability. In contrast, in the autoprotected mice, minimal downregulation of Glod4 after the high dose is likely to lead to the clearance of peroxidative by-products and adducts, thereby offering cytoresistance against oxidative stress and damage.

*Proteins involved in fatty acid transport.* FATP-2 regulates long-chain fatty acid transport across mitochondrial membranes for oxidation and release of energy in the kidney (50). With a high dose, severe downregulation of this protein leads to decreased supply of energy for the tubular epithelial cells to divide and regenerate. When the same high dose is given to primed mice, this problem no longer exists, owing to mild downregulation of FATP-2. Added to these effects, proteins involved in synthesis and maintenance of ATP are highly downregulated after the high dose, resulting in a severe compromise in cellular energy (Fig. 6). In contrast, the same proteins were mildly downregulated in the autoprotected mice (Table 3), resulting in complete recovery of ATP (Fig. 6).

*Proteins involved in protein turnover, translation elongation, and free radical scavenging.* PSA-1 has been shown to degrade abnormal proteins in the cytosol and nucleus through the ubiquitin-proteasome pathway (13, 20, 37, 44, 46, 47). The PSA-1 is the major neutral proteolytic apparatus in the cell and is an essential component of the ATP-dependent degradative pathway (20, 44, 46, 47). Recent findings suggest that inhibition of proteasome function leads to the accumulation of sufficient amounts of abnormal proteins and/or the inhibition of degradation of a key regulatory factor, e.g., heat-shock factor (6).

With the high dose of DCVC alone, PSA-1 was severely downregulated, which would be expected to result in the accumulation of undegraded anomalous proteins. These events are expected to lead to aberrant cellular signaling pathways, finally leading to increased cell death. However, when mice are primed with a low dose of DCVC, the protein turnover and repair would have been increased, leading to activation of cell survival pathways in autoprotected mice. This proposed mechanism is supported by the immunohistochemical finding of sustained presence of cytoplasmic and nuclear PSA-1 in the tubular epithelial cells in the autoprotected mice. Protein translation elongation factor is known to increase protein synthesis during repopulation of proximal tubules after injury by a single injection of $HgCl_2$ (38). In our study, we found that in low-dose and autoprotected groups, translation elongation factor was moderately downregulated, whereas with a lethal dose alone it was substantially underexpressed (Table 3), suggesting inhibition of essential protein synthesis needed for cell division and tubular repopulation of epithelial cells following high dose alone-induced injury.

It was suggested that development of oxidative stress-induced injury is prevented by PRDX5 (58). Proteomic findings in the present study revealed that downregulation of PRDX5 in low-dose and autoprotection groups was minimal (Table 3), suggesting that progression of DCVC-induced oxidative damage is curbed if the animals are primed with a low dose-stimulated tissue repair.

*DCVC-induced changes in cellular energetics.* Mitochondria are the primary targets of DCVC, thereby decreasing cellular ATP (11, 31). However, modification of specific mitochondrial proteins involved in cellular energetics after DCVC administration in animal models has not been reported. We observed that various mitochondrial precursor proteins involved in cellular respiration and ATP production are markedly downregulated with a lethal dose of DCVC alone in contrast to low-dose and autoprotected groups after DCVC. Consequently, there was severe suppression of proteins related to electron transport and ATP synthesis in the high-dose group compared with low-dose and autoprotected groups. ATP levels never recovered in the high-dose group in contrast to low-dose and autoprotected groups. Previously, we have shown that at 72 h after the low dose of DCVC, S phase DNA synthesis and renal tissue repair are at their peak (64, 65). The rapid fall in ATP levels with a low dose of DCVC at 72 h is consistent with ATP being utilized for cell division and repopulation of tubular epithelium. Increased utilization of ATP during cell division and tissue repair is well known (59). Therefore, the decline in ATP content at 72 h after low dose alone can be attributed to robust cell division and tissue repair at 72 h in response to injury inflicted at 36 h after the low dose of DCVC alone (27, 28, 64, 65), finally leading to recovery of renal structure and function. This successful repopulation of functional cells would be expected to restore the normal ATP levels as observed after an additional 36 h (108 h in Fig. 6*A*). In contrast, the same proteins that were severely downregulated with a lethal dose were only moderately downregulated if the mice

were primed with a low dose (nephron-autoprotection), meaning that their downregulation was substantially mitigated by the priming dose. In stark contrast, ATP levels recover at 72 h after the lethal dose in autoprotected mice, after repopulation of renal tubules with the new functional cells (144 h after low dose, Fig. 6*C*). Also, moderate downregulation of GRP75 in the autoprotected mice might minimize many of the morphological and functional consequences of ATP depletion.

Overall, our proteomic findings demonstrate DCVC-induced differential expression patterns of various proteins involved in critical biochemical functions related to renal injury and tissue repair mechanisms and that have functional significance in irreparable loss of renal structure and function after a high dose of DCVC in contrast to replacement and repopulation of renal tubules, leading to recovery of structure and function in autoprotected mice. These findings need further extensive validation to confirm the role of these proteins in compensatory cell division/nephrogenic repair mechanisms in the kidney to avert drug/toxicant-induced ARF.

## ACKNOWLEDGMENTS

The Colgate Palmolive Co. through the Society of Toxicology made it possible for M. C. Korrapati to conduct the experiments related to 2-dimensional electrophoresis and gel image analysis arms of proteomics in Dr. Frank A. Witzmann's laboratory.

## GRANTS

These studies were made possible through National Institute of Diabetes and Digestive and Kidney Diseases Grant DK-61650 to H. M. Mehendale. This work was partly supported by the Louisiana Board of Regents Support Fund through the University of Louisiana at Monroe, Kitty DeGree Endowed Chair in Toxicology.

## REFERENCES

1. **Abbate M, Brown D, Bonventre JV.** Expression of NCAM recapitulates tubulogenic development in kidneys recovering from acute ischemia. *Am J Physiol Renal Physiol* 277: F454–F463, 1999.
2. **Alam J, Smith A.** Heme-hemopexin-mediated induction of metallothionein gene expression. *J Biol Chem* 267: 16379–16384, 1992.
3. **Baumann H, Gauldie J.** The acute phase response. *Immunol Today* 15: 74–80, 1994.
4. **Beuter W, Cojocel C, Muller W, Donaubauer HH, Mayer D.** Peroxidative damage and nephrotoxicity of dichlorovinylcysteine in mice. *J Appl Toxicol* 9: 181–186, 1989.
5. **Bhattacharyya T, Karnezis AN, Murphy SP, Hoang T, Freeman BC, Phillips B, Morimoto RI.** Cloning and subcellular localization of human mitochondrial hsp70. *J Biol Chem* 270: 1705–1710, 1995.
6. **Bush KT, Goldberg AL, Nigam SK.** Proteasome inhibition leads to a heat-shock response, induction of endoplasmic reticulum chaperones, and thermotolerance. *J Biol Chem* 272: 9086–9092, 1997.
7. **Candiano G, Bruschi M, Musante L, Santucci L, Ghiggeri GM, Carnemolla B, Orecchia P, Zardi L, Righetti PG.** Blue silver: a very sensitive colloidal Coomassie G-250 staining for proteome analysis. *Electrophoresis* 25: 1327–1333, 2004.
8. **Carrigan PE, Nelson GM, Roberts PJ, Stoffer J, Riggs DL, Smith DF.** Multiple domains of the co-chaperone Hop are important for Hsp70 binding. *J Biol Chem* 279: 16185–16193, 2004.
9. **Chatson G, Perdrizet G, Anderson C, Pleau M, Berman M, Schweizer R.** Heat shock protects kidneys against warm ischemic injury. *Curr Surg* 47: 420–423, 1990.
10. **Chen Q, Jones TW, Brown PC, Stevens JL.** The mechanism of cysteine conjugate cytotoxicity in renal epithelial cells. Covalent binding leads to thiol depletion and lipid peroxidation. *J Biol Chem* 265: 21603–21611, 1990.
11. **Chen Y, Cai J, Anders MW, Stevens JL, Jones DP.** Role of mitochondrial dysfunction in *S*-(1,2-dichlorovinyl)-L-cysteine-induced apoptosis. *Toxicol Appl Pharmacol* 170: 172–180, 2001.
12. **Choudhary D, Chandra D, Kale RK.** Influence of methylglyoxal on antioxidant enzymes and oxidative damage. *Toxicol Lett* 93: 141–152, 1997.
13. **Ciechanover A.** The ubiquitin-proteasome proteolytic pathway. *Cell* 79: 13–21, 1994.
14. **Darnerud PO, Brandt I, Feil VJ, Bakke JE.** *S*-(1,2-dichloro-[$^{14}$C]vinyl)-L-cysteine (DCVC) in the mouse kidney: correlation between tissue-binding and toxicity. *Toxicol Appl Pharmacol* 95: 423–434, 1988.
15. **de Graauw M, Tijdens I, Cramer R, Corless S, Timms JF, van de Water B.** Heat shock protein 27 is the major differentially phosphorylated protein involved in renal epithelial cellular stress response and controls focal adhesion organization and apoptosis. *J Biol Chem* 280: 29885–29898, 2005.
16. **Emami A, Schwartz JH, Borkan SC.** Transient ischemia or heat stress induces a cytoprotectant protein in rat kidney. *Am J Physiol Renal Fluid Electrolyte Physiol* 260: F479–F485, 1991.
17. **Eskew JD, Vanacore RM, Sung L, Morales PJ, Smith A.** Cellular protection mechanisms against extracellular heme. Heme-hemopexin, but not free heme, activates the N-terminal c-jun kinase. *J Biol Chem* 274: 638–648, 1999.
18. **Esson ML, Schrier RW.** Diagnosis and treatment of acute tubular necrosis. *Ann Intern Med* 137: 744–752, 2002.
19. **Gao CX, Zhang SQ, Yin Z, Liu W.** Molecular chaperone GRP75 reprove cells from injury caused by glucose deprivation. *Shi Yan Sheng Wu Xue Bao* 36: 381–387, 2003.
20. **Goldberg AL.** Functions of the proteasome: the lysis at the end of the tunnel. *Science* 268: 522–523, 1995.
21. **Groves CE, Lock EA, Schnellmann RG.** Role of lipid peroxidation in renal proximal tubule cell death induced by haloalkene cysteine conjugates. *Toxicol Appl Pharmacol* 107: 54–62, 1991.
22. **Hernandez MP, Sullivan WP, Toft DO.** The assembly and intermolecular properties of the hsp70-Hop-hsp90 molecular chaperone complex. *J Biol Chem* 277: 38294–38304, 2002.
23. **Jaffe DR, Gandolfi AJ, Nagle RB.** Chronic toxicity of *S*-(trans-1,2-dichlorovinyl)-L-cysteine in mice. *J Appl Toxicol* 4: 315–319, 1984.
24. **Kathleen D.** Molecular mechanisms of recovery from acute renal failure. *Crit Care Med* 31: S572–S581, 2003.
25. **Kaul SC, Taira K, Pereira-Smith OM, Wadhwa R.** Mortalin: present and prospective. *Exp Gerontol* 37: 1157–1164, 2002.
26. **Kelly KJ.** Heat shock (stress response) proteins and renal ischemia/reperfusion injury. *Contrib Nephrol* 148: 86–106, 2005.
27. **Korrapati MC, Chilakapati J, Lock EA, Latendresse JR, Warbritton A, Mehendale HM.** Preplaced cell division: a critical mechanism of autoprotection against *S*-1,2-dichlorovinyl-L-cysteine-induced acute renal failure and death in mice. *Am J Physiol Renal Physiol* 291: F439–F455, 2006.
28. **Korrapati MC, Lock EA, Mehendale HM.** Molecular mechanisms of enhanced renal cell division in protection against *S*-1,2-dichlorovinyl-L-cysteine-induced acute renal failure and death. *Am J Physiol Renal Physiol* 289: F175–F185, 2005.
29. **Lameire N, Van Biesen W, Vanholder R.** Acute renal failure. *Lancet* 365: 417–430, 2005.
30. **Lameire NH, Vanholder R.** Pathophysiology of ischaemic acute renal failure. *Best Pract Res Clin Anaesthesiol* 18: 21–36, 2004.
31. **Lash LH, Anders MW.** Cytotoxicity of *S*-(1,2-dichlorovinyl)glutathione and *S*-(1,2-dichlorovinyl)-L-cysteine in isolated rat kidney cells. *J Biol Chem* 261: 13076–13081, 1986.
32. **Lee AS.** The glucose-regulated proteins: stress induction and clinical applications. *Trends Biochem Sci* 26: 504–510, 2001.
33. **Lieberthal W, Nigam SK.** Acute renal failure. II. Experimental models of acute renal failure: imperfect but indispensable. *Am J Physiol Renal Physiol* 278: F1–F12, 2000.
34. **Liebler DC.** Proteomic approaches to characterize protein modifications: new tools to study the effects of environmental exposures. *Environ Health Perspect* 110, *Suppl* 1: 3–9, 2002.
35. **Liu Y, Liu W, Song XD, Zuo J.** Effect of GRP75/mthsp70/PBP74/mortalin overexpression on intracellular ATP level, mitochondrial membrane potential and ROS accumulation following glucose deprivation in PC12 cells. *Mol Cell Biochem* 268: 45–51, 2005.
36. **Longshaw VM, Chapple JP, Balda MS, Cheetham ME, Blatch GL.** Nuclear translocation of the Hsp70/Hsp90 organizing protein mSTI1 is regulated by cell cycle kinases. *J Cell Sci* 117: 701–710, 2004.
37. **Mahaffey D, Yoo Y, Rechsteiner M.** Ubiquitin metabolism in cycling *Xenopus* egg extracts. *J Biol Chem* 268: 21205–21211, 1993.

38. **McEwen D, Ng K.** Regeneration of renal proximal tubules after mercuric chloride injury is accompanied by increased binding of aminoacyl-transfer ribonucleic acid. *Biochem J* 160: 357–365, 1976.
39. **Mene P, Polci R, Festuccia F.** Mechanisms of repair after kidney injury. *J Nephrol* 16: 186–195, 2003.
40. **Merrick BA, Bruno ME.** Genomic and proteomic profiling for biomarkers and signature profiles of toxicity. *Curr Opin Mol Ther* 6: 600–607, 2004.
41. **Merrick BA, Madenspacher JH.** Complementary gene and protein expression studies and integrative approaches in toxicogenomics. *Toxicol Appl Pharmacol* 207: 189–194, 2005.
42. **Merrick BA, Tomer KB.** Toxicoproteomics: a parallel approach to identifying biomarkers. *Environ Health Perspect* 111: A578–A579, 2003.
43. **Moshage H.** Cytokines and the hepatic acute phase response. *J Pathol* 181: 257–266, 1997.
44. **Orlowski M.** The multicatalytic proteinase complex, a major extralysosomal proteolytic system. *Biochemistry* 29: 10289–10297, 1990.
45. **Ran Q, Wadhwa R, Kawai R, Kaul SC, Sifers RN, Bick RJ, Smith JR, Pereira-Smith OM.** Extramitochondrial localization of mortalin/mthsp70/PBP74/GRP75. *Biochem Biophys Res Commun* 275: 174–179, 2000.
46. **Rivett AJ.** Proteasomes: multicatalytic proteinase complexes. *Biochem J* 291: 1–10, 1993.
47. **Rivett AJ, Knecht E.** Protein turnover: proteasome location. *Curr Biol* 3: 127–129, 1993.
48. **Rosen S, Heyman SN.** Difficulties in understanding human "acute tubular necrosis": limited data and flawed animal models. *Kidney Int* 60: 1220–1224, 2001.
49. **Satoh K, Wakui H, Komatsuda A, Nakamoto Y, Miura AB, Itoh H, Tashima Y.** Induction and altered localization of 90-kDa heat-shock protein in rat kidneys with cisplatin-induced acute renal failure. *Ren Fail* 16: 313–323, 1994.
50. **Schaffer JE, Lodish. HF.** Molecular mechanisms of long chain fatty acid uptake. *Trends Cardiovasc Med* 5: 218–224, 1995.
51. **Schober A, Muller E, Thurau K, Beck FX.** The response of heat shock proteins 25 and 72 to ischaemia in different kidney zones. *Pflügers Arch* 434: 292–299, 1997.
52. **Schrier RW, Wang W, Poole B, Mitra A.** Acute renal failure: definitions, diagnosis, pathogenesis, and therapy. *J Clin Invest* 114: 5–14, 2004.
53. **Shangari N, O'Brien PJ.** The cytotoxic mechanism of glyoxal involves oxidative stress. *Biochem Pharmacol* 68: 1433–1442, 2004.
54. **Shevchenko A, Wilm M, Vorm O, Mann M.** Mass spectrometric sequencing of proteins silver-stained polyacrylamide gels. *Anal Chem* 68: 850–858, 1996.
55. **Singri N, Ahya SN, Levin ML.** Acute renal failure. *JAMA* 289: 747–751, 2003.
56. **Smith A, Alam J, Escriba PV, Morgan WT.** Regulation of heme oxygenase and metallothionein gene expression by the heme analogs, cobalt-, and tin-protoporphyrin. *J Biol Chem* 268: 7365–7371, 1993.
57. **Smoyer WE, Ransom R, Harris RC, Welsh MJ, Lutsch G, Benndorf R.** Ischemic acute renal failure induces differential expression of small heat shock proteins. *J Am Soc Nephrol* 11: 211–221, 2000.
58. **Soini Y, Kallio JP, Hirvikoski P, Helin H, Kellokumpu-Lehtinen P, Kang SW, Tammela TL, Peltoniemi M, Martikainen PM, Kinnula VL.** Oxidative/nitrosative stress and peroxiredoxin 2 are associated with grade and prognosis of human renal carcinoma. *APMIS* 114: 329–337, 2006.
59. **Soni MG, Mehendale HM.** Adenosine triphosphate protection of chlordecone-amplified CCl4 hepatotoxicity and lethality. *J Hepatol* 20: 267–274, 1994.
60. **Stacchiotti A, Lavazza A, Rezzani R, Borsani E, Rodella L, Bianchi R.** Mercuric chloride-induced alterations in stress protein distribution in rat kidney. *Histol Histopathol* 19: 1209–1218, 2004.
61. **Thornalley PJ.** The glyoxalase system: new developments towards functional characterization of a metabolic pathway fundamental to biological life. *Biochem J* 269: 1–11, 1990.
62. **Tolosano E, Hirsch E, Patrucco E, Camaschella C, Navone R, Silengo L, Altruda F.** Defective recovery and severe renal damage after acute hemolysis in hemopexin-deficient mice. *Blood* 94: 3906–3914, 1999.
63. **Ueda N, Kaushal GP, Shah SV.** Apoptotic mechanisms in acute renal failure. *Am J Med* 108: 403–415, 2000.
64. **Vaidya VS, Shankar K, Lock EA, Bucci TJ, Mehendale HM.** Renal injury and repair following *S*-1, 2 dichlorovinyl-L-cysteine administration to mice. *Toxicol Appl Pharmacol* 188: 110–121, 2003.
65. **Vaidya VS, Shankar K, Lock EA, Bucci TJ, Mehendale HM.** Role of tissue repair in survival from *S*-(1,2-dichlorovinyl)-L-cysteine-induced acute renal tubular necrosis in the mouse. *Toxicol Sci* 74: 215–227, 2003.
66. **Vaidya VS, Shankar K, Lock EA, Dixon D, Mehendale HM.** Molecular mechanisms of renal tissue repair in survival from acute renal tubule necrosis: role of ERK1/2 pathway. *Toxicol Pathol* 31: 604–618, 2003.
67. **Van Der Spuy J, Kana BD, Dirr HW, Blatch GL.** Heat shock cognate protein 70 chaperone-binding site in the co-chaperone murine stress-inducible protein 1 maps to within three consecutive tetratricopeptide repeat motifs. *Biochem J* 345: 645–651, 2000.
68. **Van Why SK, Hildebrandt F, Ardito T, Mann AS, Siegel NJ, Kashgarian M.** Induction and intracellular localization of HSP-72 after renal ischemia. *Am J Physiol Renal Fluid Electrolyte Physiol* 263: F769–F775, 1992.
69. **Venkatachalam MA, Rennke HG, Sandstrom DJ.** The vascular basis for acute renal failure in the rat. Preglomerular and postglomerular vasoconstriction. *Circ Res* 38: 267–279, 1976.
70. **Vidal BC, Bonventre JV, I-Hong-Hsu S.** Towards the application of proteomics in renal disease diagnosis. *Clin Sci (Lond)* 109: 421–430, 2005.
71. **Wadhwa R, Taira K, Kaul SC.** An Hsp70 family chaperone, mortalin/mthsp70/PBP74/Grp75: what, when, and where? *Cell Stress Chaperones* 7: 309–316, 2002.
72. **Wadhwa R, Taira K, Kaul SC.** Mortalin: a potential candidate for biotechnology and biomedicine. *Histol Histopathol* 17: 1173–1177, 2002.
73. **Wadhwa R, Yaguchi T, Hasan MK, Mitsui Y, Reddel RR, Kaul SC.** Hsp70 family member, mot-2/mthsp70/GRP75, binds to the cytoplasmic sequestration domain of the p53 protein. *Exp Cell Res* 274: 246–253, 2002.
74. **Wetmore BA, Merrick BA.** Toxicoproteomics: proteomics applied to toxicology and pathology. *Toxicol Pathol* 32: 619–642, 2004.